# Using FUN3D for Aeroelastic, Sonic Boom, and AeroPropulsoServoElastic (APSE) Analyses of a Supersonic Configuration

Walter A. Silva,* Mark D. Sanetrik,† and Pawel Chwalowski‡
*NASA Langley Research Center, Hampton, Virginia*

Joseph Connolly§ and George Kopasakis¶
*NASA Glenn Research Center Cleveland, Ohio*

**An overview of recent applications of the FUN3D CFD code to computational aeroelastic, sonic boom, and aeropropulsoservoelasticity (APSE) analyses of a low-boom supersonic configuration is presented. The overview includes details of the computational models developed including multiple unstructured CFD grids suitable for aeroelastic and sonic boom analyses. In addition, aeroelastic Reduced-Order Models (ROMs) are generated and used to rapidly compute the aeroelastic response and flutter boundaries at multiple flight conditions.**

## I. Introduction

A top priority for the Commercial Supersonic Technology (CST) project under the ASE (aeroservoelasticity) element is to develop the tools required to perform accurate, high fidelity computational aeroelasticity (AE), aeroservoelastic (ASE), and aeropropulsoservoelasticity (APSE) analyses in support of the design of future low-boom high-speed civil aircraft. As a means of accomplishing that priority, the CST project is working with Lockheed-Martin to conduct such analyses. Under the NASA N+2 (two generations from present state) contract, Lockheed-Martin developed a low-boom supersonic configuration and a detailed finite element model (FEM) of the vehicle. An artist rendering of the Lockheed-Martin N+2 configuration is presented in Figure 1. The goal of the N+2 effort is to develop and validate technologies for future civil supersonic airliners.

Figure 1: Artist's concept of the Lockheed-Martin N+2 configuration.

*Senior Research Scientist, Aeroelasticity Branch, AIAA Associate Fellow.
†Aerospace Engineer, Aeroelasticity Branch.
‡Aerospace Engineer, Aeroelasticity Branch.
§Aerospace Engineer, Intelligent Control and Autonomy Branch.
¶Aerospace Engineer, Intelligent Control and Autonomy Branch.

In addition to the aeroelastic and sonic boom analyses of the N+2 configuration, the CST Project's ASE element is also involved in the development of APSE models. The development of an APSE model consists of the interconnection of a traditional ASE model (airframe model) with a dynamic engine model. Traditionally, these two models are developed and used separately by distinct disciplines (such as ASE and propulsion performance). The ultimate goal of this development effort is to be able to determine if airframe flexibility has an effect on the thrust dynamics of the propulsion system. To achieve this goal, a propulsion system model will be coupled to the airframe flexibility modes in a closed-loop system, thereby enabling an analysis of their combined effect on vehicle performance.

This paper presents a status update on this computational effort.[1,2] This includes a description of the N+2 configuration and a summary of the Lockheed-Martin finite element model (FEM). Euler (inviscid) and Navier-Stokes (viscous) results that address the effect of static aeroelastic deformation on sonic boom propagation are presented. Reduced-Order Model (ROM) solutions at multiple flight conditions are presented and discussed. Finally, recent progress regarding the development of a FUN3D-based APSE model is discussed.

## II. Unstructured Grids

Unstructured grids of the N+2 configuration have been generated for use with the FUN3D code.[3] Additional details regarding the aeroelastic capability within the FUN3D code can be found in the reference.[4]

Recent work has focused on the creation of improved grids that are better suited for sonic boom propagation. Given that the grids generally used for aeroelastic analyses are not well suited for modeling sonic boom propagation, several parametric studies have been performed in order to develop the best possible grids for both aeroelastic and sonic boom propagation analyses. Presented in Figure 2 is a close-up detail of the grid used for standard computational aeroelastic analyses. As can be seen, the generation of a grid for aeroelastic analysis does not, typically, include tailoring the grid to capture supersonic bow shocks. Generally speaking, a grid generated for computational aeroelastic analyses can be used for computing solutions at multiple Mach numbers. Given that the primary focus of the aeroelastic analyses is the unsteady surface pressures and the resultant integrated forces, the emphasis of the quality of the grid is focused on the surface of the vehicle.

Grids for sonic boom prediction are aligned to the Mach angle and stretched to reduce dissipation so that pressure signatures can be computed off-body. The off-body signatures are then processed using the sonic boom propagation software SBOOM[5] to compute the propagation of the off-body signature to the ground level.

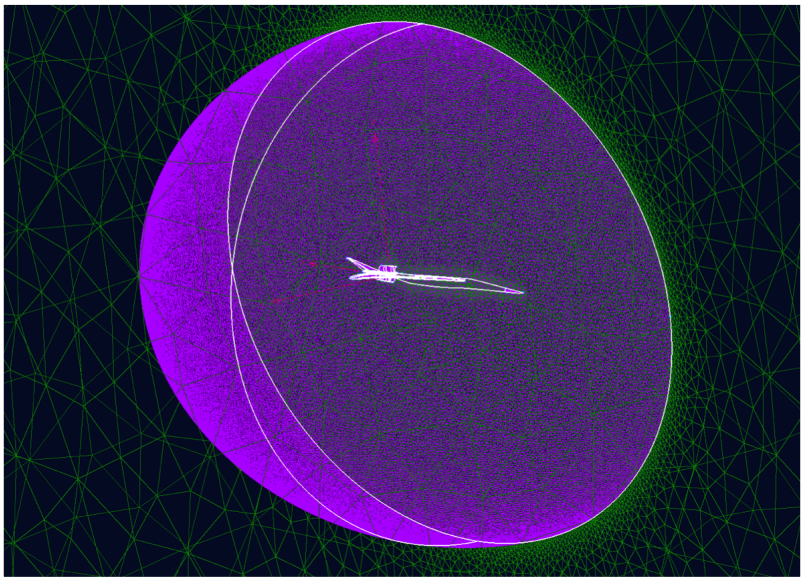

Figure 2: Close-up of the grid used for aeroelastic analyses.

Figure 3 shows the steady aerodynamic flow computed using the conventional aeroelastic analysis grid at a Mach number of 1.7 and angle of attack of 2.25 degrees. As can be seen, the bow shocks are not well resolved

for this solution even with the use of a grid with approximately 12 million grid points. Clearly, the grids that are typically used for computational aeroelastic analysis are not appropriate for the computation of the effect of static aeroelastic response on sonic boom propagation. For this type of analyses, it is appropriate to generate grids suitable for computing the propagation of the sonic boom and then use these grids for computational aeroelastic analyses.

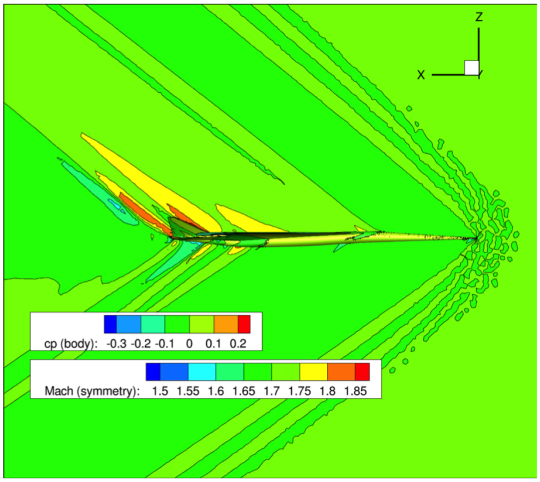


Figure 3: Steady aerodynamic solution for sonic boom propagation analysis using grid generated for aeroelastic analyses.

Multiple grids were generated for sonic boom propagation studies with grid dimensions of 16 million grid points (coarse), 45 million grid points (medium), and 90 million grid points (fine). An additional variation considered the effect of the engines on both the sonic boom propagation and the aeroelastic response. The engine masses are, of course, still included in the structural dynamic model of the vehicle. The results presented in the remainder of this section consist of computations at the cruise condition (Mach number of 1.7 and alpha = 2.25 degrees) using grids that were generated without the engines.

Presented in Figure 4 is the static aeroelastic deformation of the entire vehicle at the cruise condition due to an inviscid aerodynamic solution. Although the deformation is not large, it can be seen that it does occur over a large portion of the vehicle. This will have an impact on the sonic boom propagation.

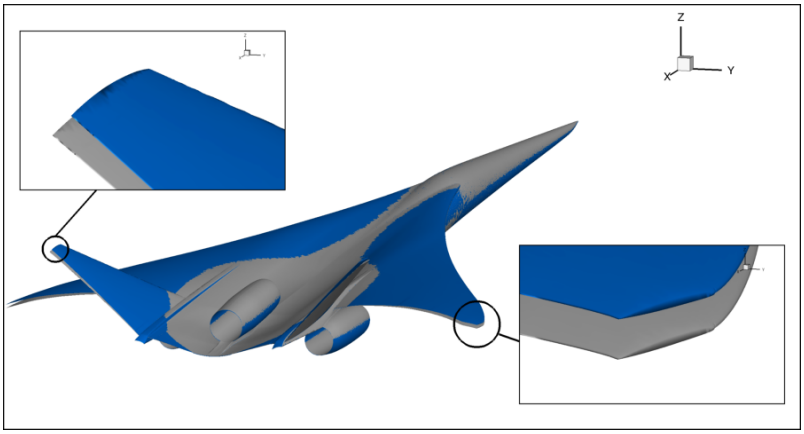


Figure 4: Static aeroelastic deformation of the N+2 configuration at cruise. Gray is undeformed; Blue is deformed.

Figure 5 presents the coarse grid used for sonic boom propagation. The challenge in generating grids for sonic boom propagation analyses is that a separate grid needs to be generated for each condition of interest (Mach number and angle of attack). This complexity adds significant overhead to the overall analysis but, is

essential for obtaining accurate results. Subsequent computational aeroelastic analyses are then performed using each one of the sonic boom propagation grids.

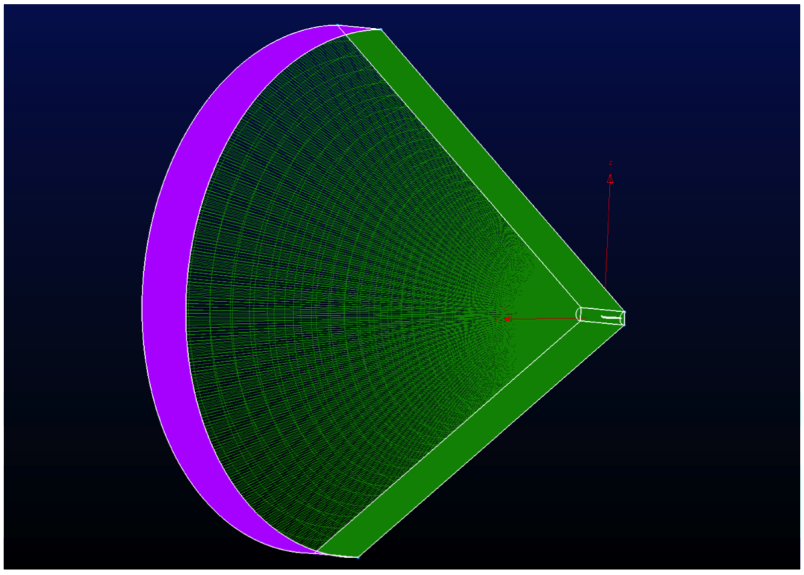

Figure 5: Sample coarse grid used for conducting a sonic boom propagation analysis.

Figure 6 shows the steady aerodynamic flow Mach number at the cruise condition determined using the coarse sonic boom grid without the engines. As can be seen, the bow shocks are better resolved using this grid compared to the grid generated for aeroelastic analyses. Presented in Figure 7 is a close-up view of Figure 6 showing the improved resolution of the bow shocks.

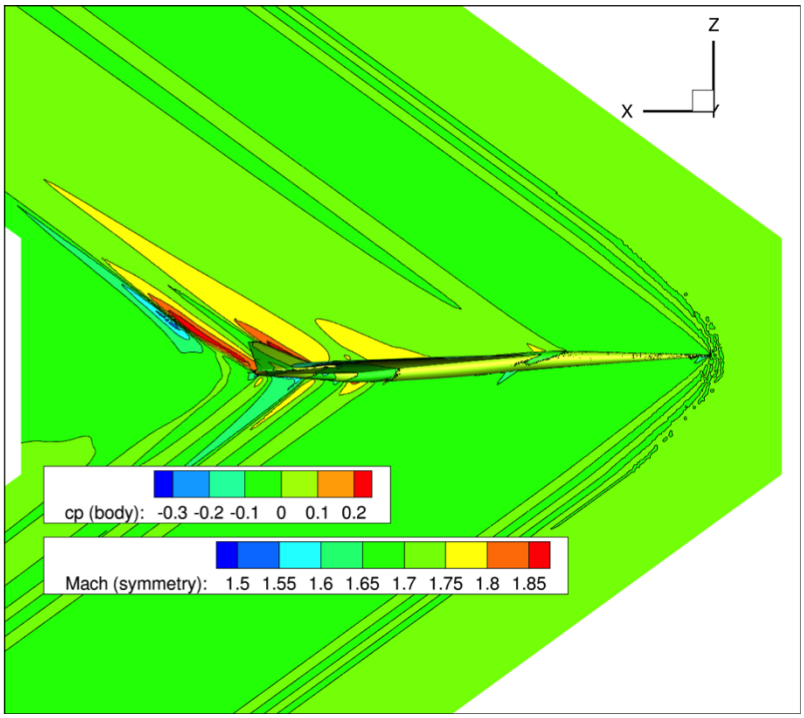


Figure 6: Steady aerodynamic solution for sonic boom propagation analysis using the coarse grid.

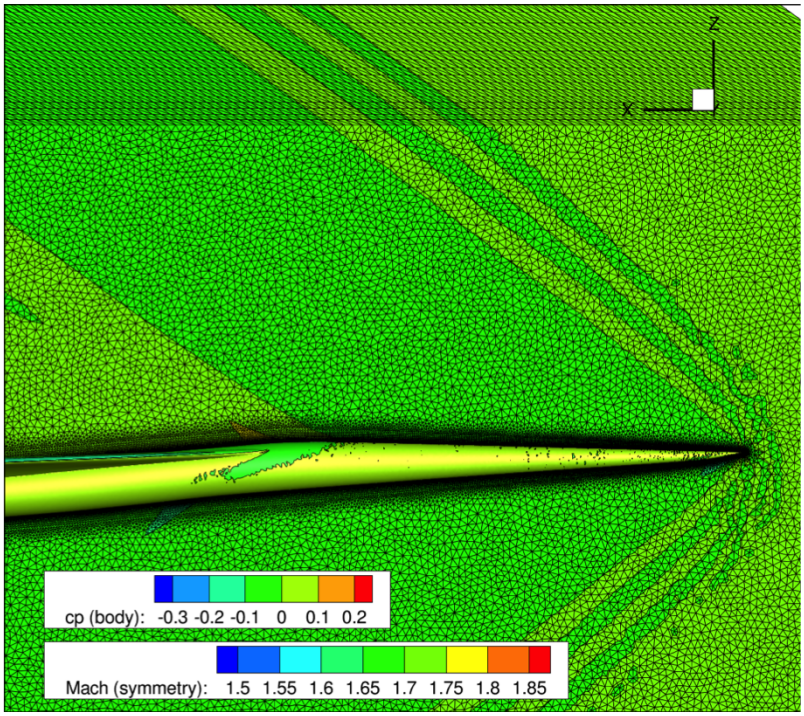


Figure 7: Close-up detail of the bow shocks for sonic boom analysis using the coarse grid.

Shown in Figure 8 and in Figure 9 is the steady aerodynamic flow Mach number at the cruise condition using the medium and fine sonic boom grids, respectively, both without the engines. Clearly, resolution of the grid significantly improves the resolution of the bow shocks which leads to improved accuracy with respect to sonic boom propagation.

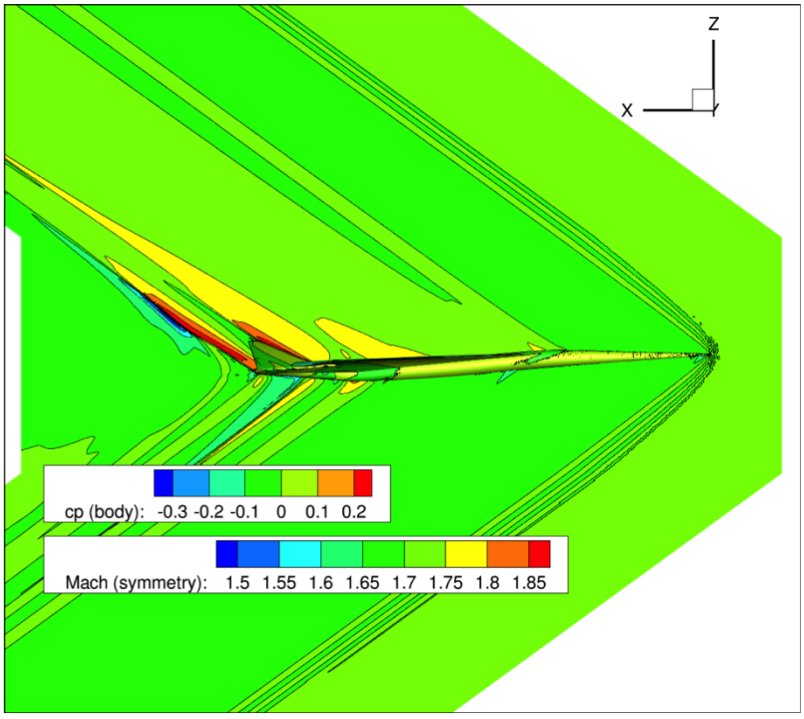


Figure 8: Steady aerodynamic solution for sonic boom propagation analysis using the medium grid.

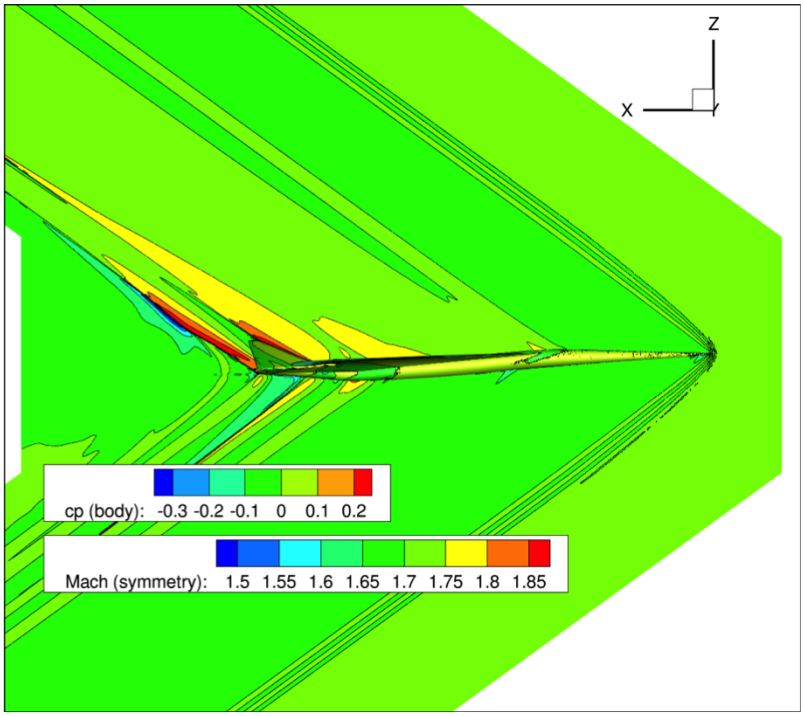


Figure 9: Steady aerodynamic solution for sonic boom propagation analysis using the fine grid.

Figure 10 presents a comparison of the ground level boom signature for the three different grid densities for the configuration with no engines at the cruise condition. As can be seen, use of the finer grid exhibits some variation near the middle of the signature not seen with the coarse and medium density grids.

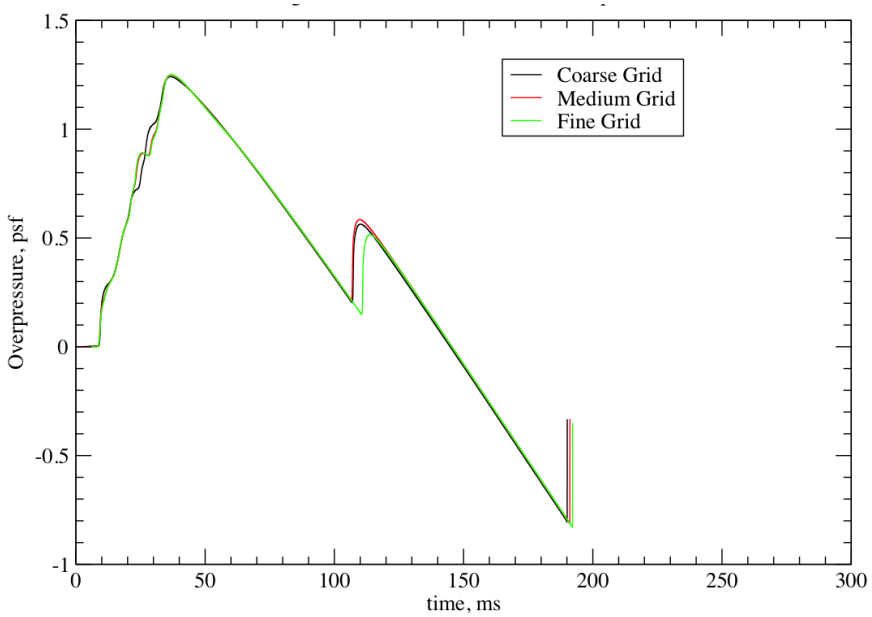


Figure 10: Ground-level boom signature at cruise for various grid densities.

Presented in Figure 11 is a comparison of the ground-level boom signature for the undeformed configurations, with and without engines at the cruise condition. As can be seen, inclusion of the engines in the aerodynamic solution clearly exhibits some variation near the middle of the signature. This difference is

not surprising and is intended to serve as a basis for comparison with the deformed configuration (with and without engines), to be presented in a subsequent paper.

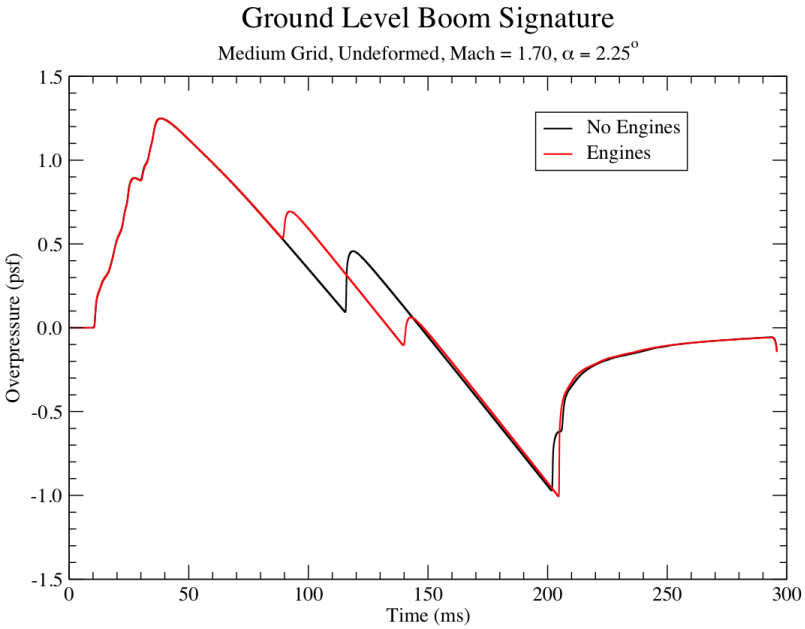


Figure 11: Effect of engine presence on ground-level boom signature at cruise, undeformed case, medium grid.

Presented in Figure 12 is a comparison of the ground-level boom signature for the undeformed and deformed conditions for the configuration with no engines at the cruise condition. There is clearly an effect of the static aeroelastic deflection on the ground-level boom signature. However, additional analysis is required to better understand the implications of this result.

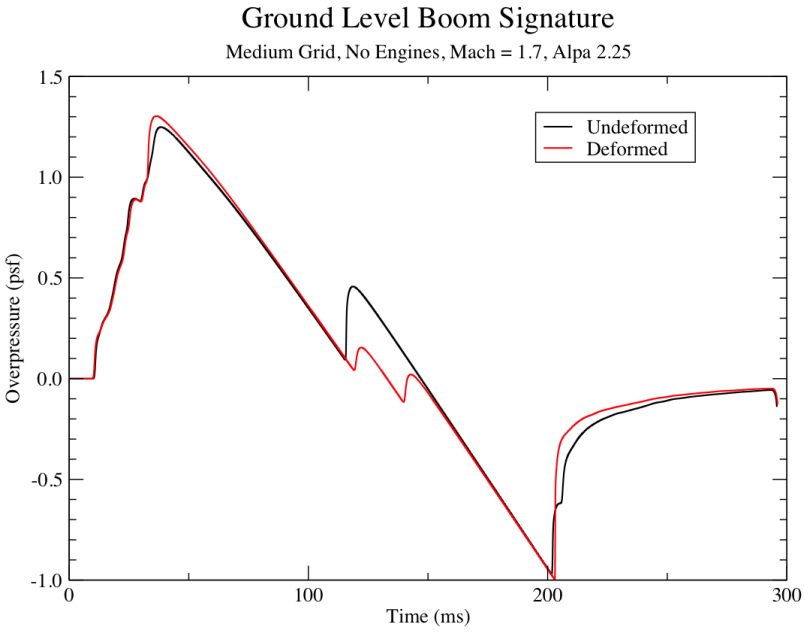


Figure 12: Ground-level boom signature at cruise for the undeformed and deformed cases.

## III. Reduced-Order Models

The goal behind the development of a ROM for the rapid computation of unsteady aerodynamic and aeroelastic responses is aimed at addressing two challenges. The first challenge is the computational cost associated with full CFD aeroelastic simulations, which increases with the fidelity of the nonlinear aerodynamic equations to be solved as well as the complexity of the configuration. Computational cost, however, may be reduced via the implementation of parallel processing techniques, advanced algorithms, and improved computer hardware processing speeds.

The second, more serious, challenge is that the information generated by these simulations cannot be used effectively within a preliminary design environment. Because the output of these full CFD aeroelastic simulations, such as the responses of the generalized coordinates, is not easily incorporated within a design environment, parametric variations and design studies can only be performed by trial-and-error. As a result, the integration of computational aeroelastic simulations into preliminary design activities involving disciplines such as aeroelasticity, aeroservoelasticity (ASE), and optimization continues to be a costly and impractical venture.

However, with the development of reduced-order modeling (ROM) methods,[6,7] the rapid generation of root locus plots using CFD-based unsteady aerodynamics is now available to aeroelasticians. This recently developed technology is being applied to the N+2 supersonic configuration for evaluation of aeroelastic mechanisms across several Mach numbers. A sample of some of those results is presented in the following.

Aeroelastic ROMs have been developed at a Mach number of 1.7, 1.05, and 0.98. Presented in Figure 13 is a comparison of the dynamic aeroelastic response from a full FUN3D aeroelastic solution and the ROM aeroelastic solution at a Mach number of 1.7 and a dynamic pressure of 2.149 psi where the time histories of the fourth mode generalized displacements are compared. As can be seen, the results are practically identical. Similar results are obtained for all the other modes, indicating good confidence in the ROM.

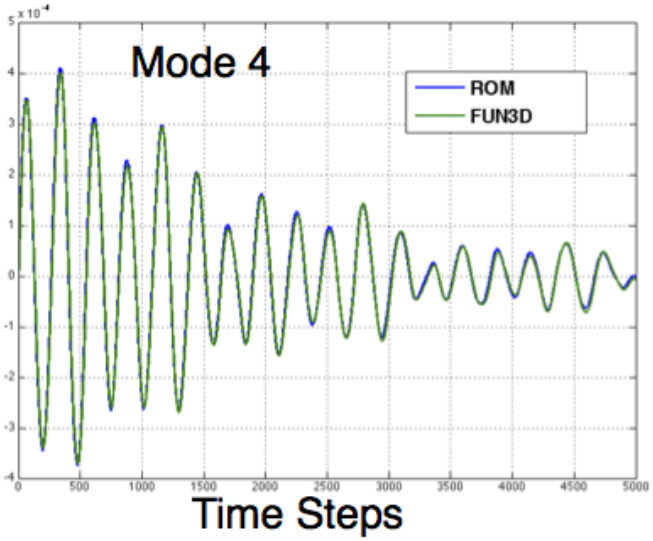


Figure 13: Comparison of full FUN3D aeroelastic response and ROM aeroelastic response for the fourth mode at M=1.7 and a dynamic pressure of 2.149 psi.

A major benefit of this ROM technology is the ability to rapidly generate an aeroelastic root locus plot that reveals the aeroelastic mechanisms occurring at that flight condition. Presented in Figure 14 is the aeroelastic root locus plot at M=0.98 with a variation in dynamic pressure from 1 to 20 psi, with the arrows indicating increasing dynamic pressure. Potential coalescence between modes is evident, including a softening of the first flexible mode. This softening of the first mode could indicate a tendency towards body freedom flutter if it couples with the short period mode. In Figure 15, the aeroelastic root locus plot at M=1.05 indicates an interesting variation of the first mode as it starts out moving in a stable direction (towards the left) and then reverses direction and moves towards the right, eventually crossing the imaginary axis (flutter). Both root loci plots have the same maximum dynamic pressure of 20 psi. The increased variation of the solution at M=1.05 indicates a greater sensitivity to flutter than at other Mach numbers thus far. Additional analyses are underway to determine the significance of this modal variation. Regardless, the flutter event is still significantly outside of the flight envelope of the N+2 configuration.

The computational cost of generating these ROM solutions consists of one full FUN3D solution that is used to generate the ROM at that Mach number. Each full FUN3D solution ran for about three hours and consisted of 2400 time steps. Once this solution is available, a ROM can be generated and then used to generate all the aeroelastic responses at all dynamic pressures. In comparison, a full FUN3D analysis at each dynamic pressure requires two full FUN3D solutions: a static aeroelastic (10 hours) and a dynamic aeroelastic (18 hours). Therefore, full FUN3D solutions for 20 dynamic pressures would require 560 hours of compute time.

In the root locus plot, each symbol represents the aeroelastic roots at a specific dynamic pressure. It is important to mention that this ROM-based root locus plot is generated in seconds while multiple full FUN3D solutions would be required for each dynamic pressure of interest to generate an equivalent full FUN3D solution root locus.

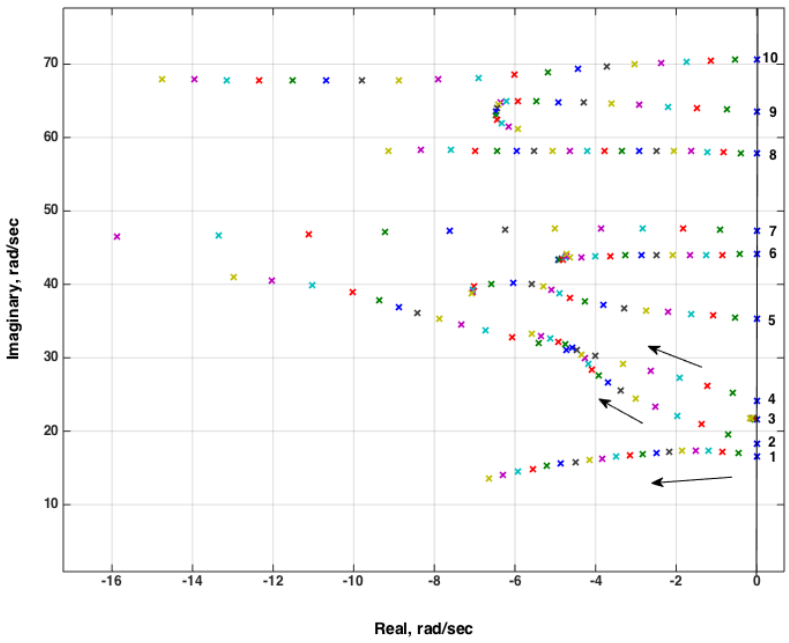


Figure 14: Aeroelastic root locus plot at M=0.98.

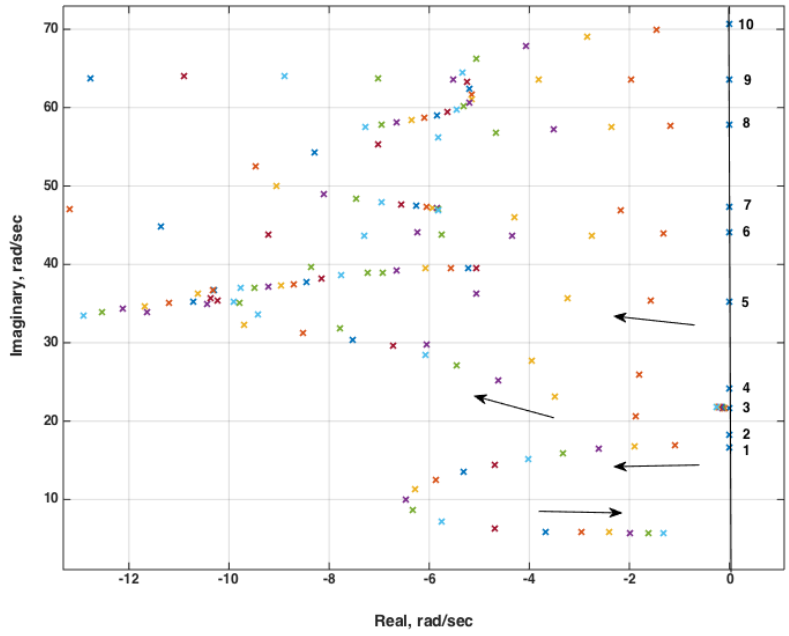


Figure 15: Aeroelastic root locus plot for the cruise condition at M=1.05.

## IV. AeroPropulsoServoElasticity

To conduct the APSE studies, the propulsion system model needs to be integrated into a CFD solver, such as FUN3D, that is capable of modeling aeroelastic effects of a commercial supersonic vehicle. Up until

now, FUN3D could simulate inlet and nozzle flows, but not the effect of any turbo machinery components that may influence those flows. An air breathing propulsion simulation in FUN3D is currently constrained to independently specified boundary conditions at an engine inlet and exit plane. At the inlet plane, the static pressure ratio is specified. At the exit plane, total pressure and total temperature is specified according to whether the exit plane is within the subsonic plenum of the nozzle or downstream of the throat in the supersonic section.

Current efforts have allowed for a previously developed Variable Cycle Engine (VCE) that will provide a new capability by creating a C code library of the engine model that can be read by FUN3D at simulation startup. The current proof-of-concept configuration is a fully 3D engine nacelle with an external compression axi-symmetric inlet and a three-flow path convergent-divergent nozzle. These two complicated component models are connected by the quasi 1D C-library VCE model. The engine model uses the average total pressure and temperature from the solution at the engine inlet plane coming from the 3D flow solver and calculates the nozzle exit-plane boundary conditions.

Previously, propulsion systems in FUN3D just modeled the place in the simulation for the gas turbine engine as a hollow tube. This new feature now allows for the accurate propagation of the flow condition at the engine inlet boundary to theexit boundary within the nozzle. A preliminary result of the steady-state Mach number contours is shown in Figure 16. This preliminary result illustrates the Mach number of 1.7, 50,000ft, and 100% power condition and exhibits the expected main features of the flow field with a normal shock near the inlet cowl and the nozzle flow capturing the complex interactions of the various speed of the flow exiting the nozzle. On-going work is needed to gain certainty of the results, however the main goal of interfacing the two simulation environments was achieved.

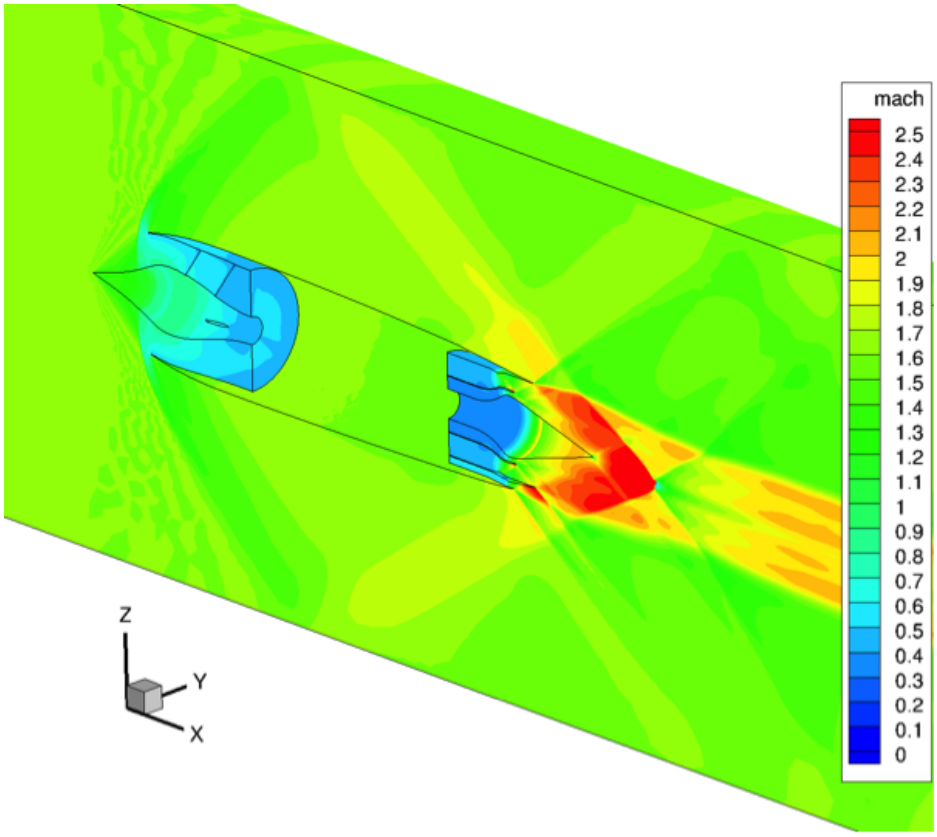


Figure 16: Steady-state Mach number contours (preliminary results) of the FUN3D propulsion system using the VCE model at Mach 1.7, 50,000 ft., and 100% power condition.

Additional work is currently underway to investigate the unsteady behavior of the simulation before using this new capability in APSE studies. As part of this work, the VCE engine model was integrated into a 3D simulation of the full N+2 configuration, as shown in Figure 17. Preliminary results indicate that a steady

solution can be obtained for this more complex configuration. However, computing fully unsteady solutions (pitching, for example) and aeroelastic solutions will require additional model development.

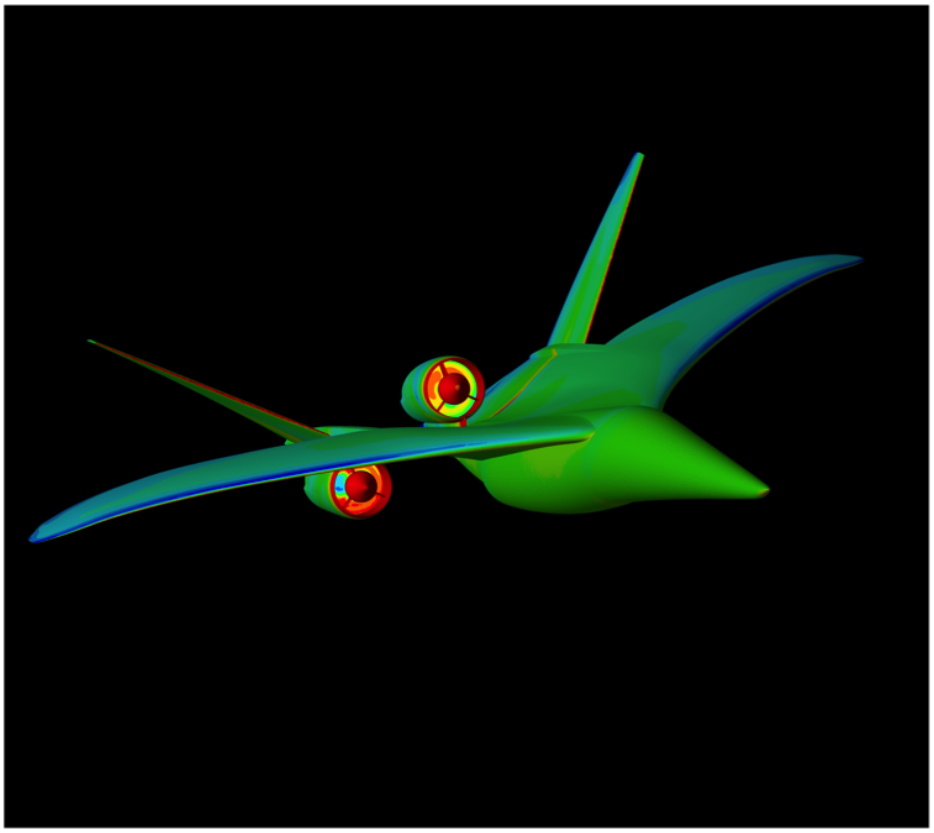

Figure 17: FUN3D simulation result with VCE lumped-volume propulsion model for the full N+2 configuration.

## V. Concluding Remarks

A status review for the ASE project under the CST Program was presented. Results presented included computational aeroelastic and sonic boom propagation analysis using the FUN3D CFD code. These results indicated that the use of a fine grid is necessary for accurate sonic boom propagation analysis. Aeroelastic root locus plots generated using ROMs at three Mach numbers were presented as well. Based on these root locus plots, there are indications that the aeroelastic mechanisms exhibit some variance across Mach numbers. Finally, recent progress in the development of an APSE model, embedded within the FUN3D code, shows good progress.

## References


[1]Silva, W. A., Garza, A. D. L., Zink, P. S., Bounajem, E., Johnson, C., Buonanno, M., Sanetrik, M. D., Yoo, S., Kopasakis, G., and Christhilf, D. M., "The NASA High Speed ASE Project: Computational Analyses of a Low-Boom Supersonic Configuration," *55th AIAA/ASMe/ASCE/AHS/SC Structures, Structural Dynamics, and Materials Conference*, No. 2014-0675, Jan. 2014.

[2]Silva, W. A., Garza, A. D. L., Zink, P. S., Bounajem, E., Johnson, C., Buonanno, M., Sanetrik, M. D., Chwalowski, P., Y.Yoo, S., and Hur, J., "An Overview of the NASA High Speed ASE Project: Aeroelastic Analyses of a Low-Boom Supersonic Configuration," *56th AIAA/ASCE/AHS/SC Structures, Structural Dynamics, and Materials Conference*, No. 2015-0684, Jan. 2015.

[3]Biedron, R. T. and Thomas, J., "Recent Enhancements to the FUN3D Flow Solver for Moving-Mesh Applications," *47th AIAA Aerospace Sciences Meeting*, No. 2009-1360, Orlando, FL, Jan. 5-8 2009.

[4]Biedron, R. T. and Thomas, J. L., "Recent Enhancements to the FUN3D Flow Solver for Moving Mesh Applications," *47th AIAA Aerospace Sciences Meeting, Orlando, FL*, January 2009.

[5]Rallabhandi, S. K., "Advanced Sonic Boom Prediction Using Augmented Burger's Equation," *Journal of Aircraft*, Vol. 48, No. 4, September-October 1993, pp. 1245–1253.

[6]Silva, W. A., "Simultaneous Excitation of Multiple-Input/Multiple-Output CFD-Based Unsteady Aerodynamic Systems," *Journal of Aircraft*, Vol. 45, No. 4, July-August 2008, pp. 1267–1274.

[7]Silva, W. A., Vatsa, V. N., and Biedron, R. T., "Reduced-Order Models for the Aeroelastic Analyses of the Ares Vehicles," AIAA Paper No. 2010-4375, presented at the 28th AIAA Applied Aerodynamics Conference, Chicago, IL.